Spectral properties and laser performance of $Nd:Lu_3Al_5O_{12}$ ceramic

Shuqi Qiao (乔书旗)[1,†], Yang Zhang (张 阳)[2,†], Xiangchun Shi (施翔春)[1,*], Benxue Jiang (姜本学)[2,], Long Zhang (张 龙)[2], Xiaojin Cheng (程小劲)[1], Lei Li (李 磊)[1], Jianlei Wang (王建磊)[1], and Luo Gui (桂 珞)[1]**

[1]*Key Laboratory of Space Laser Communication and Detection Technology, Shanghai Institute of Optics and Fine Mechanics, Chinese Academy of Sciences, Shanghai 201800, China*

[2]*Key Laboratory of High Power Laser Materials, Shanghai Institute of Optics and Fine Mechanics, Chinese Academy of Sciences, Shanghai 201800, China*

**Corresponding author: shixc@siom.ac.cn; **corresponding author: jiangsic@foxmail.com*

Received February 6, 2015; accepted March 16, 2015; posted online April 24, 2015

In this work, the absorption, fluorescence spectra, and fluorescence decay curve of $Nd:Lu_3Al_5O_{12}$, i.e., neodymium lutetium aluminum garnet (Nd:LuAG) ceramic are investigated. A diode-end-pumped Nd:LuAG ceramic laser is demonstrated for the first time (to our knowledge). We present the experiment results of Nd:LuAG ceramic's continuous wave (CW) and electro-optically (E-O) Q-switched performance. CW output power of 2.5 W is obtained, corresponding to optical-to-optical efficiency of 17.2% and slope efficiency of 24.3%. For the E-O Q-switched setup, the shortest pulse width and the largest pulse energy are measured to be 4.8 ns and 1.96 mJ, respectively. Its optical-to-optical efficiency and the slope efficiency are 17.3% and 28.7%, respectively.

OCIS codes: 160.3380, 140.3380, 140.3480, 140.3530.
doi: 10.3788/COL201513.051602.

Lutetium aluminum garnet (LuAG) has attracted a great deal of attention as one of the most attractive laser hosts due to its excellent physical and chemical properties[1,2]. Compared with $Nd:Y_3Al_5G_{12}$ (Nd:YAG), Nd:LuAG has longer fluorescence lifetime and larger saturation fluence, which makes it a promising material to apply in high-energy lasers. There are some reports about Nd:LuAG crystal lasers. Continuous wave (CW) and passively Q-switched performances of Nd:LuAG crystal were demonstrated[3–6]. Compared with crystal, ceramic has many outstanding features in the application of high-energy lasers: easily fabricated, much larger size, and high doping concentration. Meanwhile, ceramic also has other advantages, namely: less expensive, and available as a multilayer and multi-functional material. Since Ikesue *et al.* reported that the fabrication of Nd^{3+}-doped YAG laser ceramics with excellent optical quality and laser output[7], Nd:YAG ceramic has attracted considerable attention. In 2014, Chen *et al.* investigated a quasi-continuous-wave (QCW) face-pumped Nd:YAG ceramic laser and achieved 4.35 kW output power, corresponding to an optical-to-optical efficiency of 43.6%[8]. But, until now, neither CW nor electro-optically (E-O) Q-switch laser output of the Nd:LuAG ceramic have been achieved. In this Letter, we report, to the best of our knowledge, the first demonstration of laser output which use Nd:LuAG ceramic as the laser gain medium.

Laser material is one of the most significant research issues for inertial fusion energy (IFE) driver developments. The preferable emission cross section of the IFE gain medium is between 2×10^{-20} and 7×10^{-20} cm^2[9], which is close to that of Nd:LuAG ceramic. All results indicate that Nd:LuAG ceramic is a promising material to apply in IFE laser system. Meanwhile, high-energy lasers have been widely used in space applications[10–12].

In our work, the Nd:LuAG ceramic was fabricated by vacuum sintering plus hot isostatic press (HIP) sintering method[13].

The room-temperature absorption and emission spectrum of Nd:LuAG ceramic are shown in Figs. 1(a) and 1(b), respectively. The thickness of sample used in this experiment is 5 mm. The transitions $^4I_{9/2} \rightarrow {}^2L_{15/2} + {}^4D_{1/2} + {}^2I_{11/2} + {}^4D_{5/2} + {}^4D_{3/2}$, $^4I_{9/2} \rightarrow {}^4G_{5/2} + {}^2G_{7/2}$, $^4I_{9/2} \rightarrow {}^4F_{7/2} + {}^4S_{3/2}$, and $^4I_{9/2} \rightarrow {}^2H_{9/2} + {}^4F_{5/2}$ around 355, 589, 748, and 808 nm, respectively, are prominent. The absorption band at 808 nm has a full-width half-maximum (FWHM) of 5 nm, which is suitable for AlGaAs diode-laser pumping.

We also measured the transmission of Nd:LuAG ceramic from 1000 to 1100 nm. We can get that the average transmission is 83.01% when 5 mm thick Nd:LuAG ceramic was measured. According to the Fresnel formula $R = \frac{(n-1)^2}{(n+1)^2}$, we can deduce the transmission formula

$$T = \frac{(1-R)^2 \times \exp(-\alpha/2)}{1 - [R \times \exp(-\alpha/2)]^2}, \tag{1}$$

where n is the refractive index (1.824) of the Nd:LuAG ceramic at 1064 nm, R is the reflectivity of Nd:LuAG ceramic at 0° incident, and α is the scattering loss of 1 cm. We can get that the scattering loss of Nd:LuAG ceramic is 0.0306 cm^{-1}. The fluorescence spectrum of

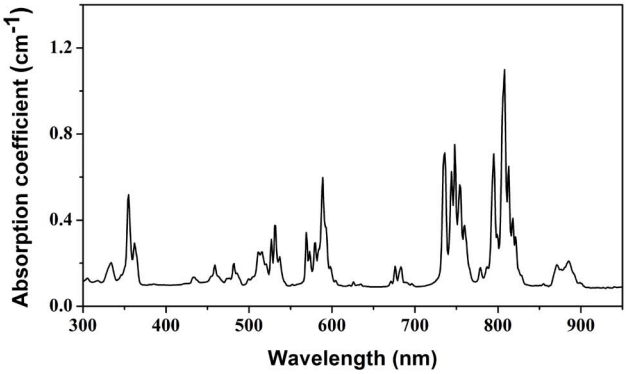

(a)

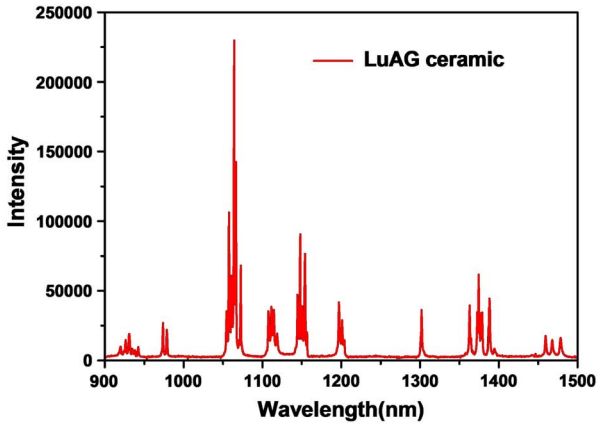

(b)

Fig. 1. Spectra of Nd:LuAG ceramic at room temperature; (a) absorption; (b) emission.

Nd:LuAG ceramics in the range 900–1500 nm is shown in Fig. 1(b). Three emission bands corresponding to the $^4F_{3/2} \rightarrow {}^4I_{9/2}$, $^4I_{11/2}$, and $^4I_{13/2}$ transitions are observed at 910–980, 1050–1210, and 1300–1480 nm, respectively. The most intense peaks are at 1066 nm.

Fluorescence decay curve for the $^4F_{3/2} \rightarrow {}^4I_{11/2}$ energy transition is shown in Fig. 2. The decay time was measured by a computer-controlled transient digitizer. The curve follows nearly single-exponential decay behavior.

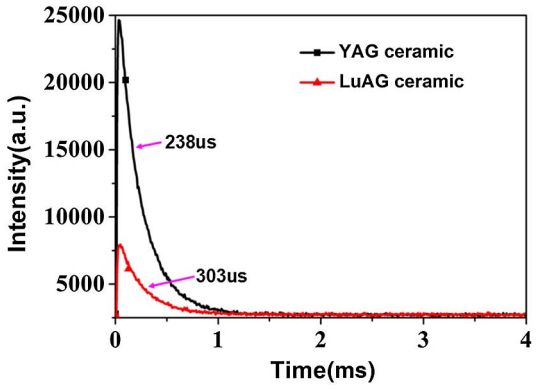

Fig. 2. Fluorescence decay curve of the $^4F_{3/2}$ multiplet in Nd:LuAG and Nd:YAG ceramics.

The fluorescence lifetime of Nd:LuAG and Nd:YAG transparent ceramics were fitted to be 303 and 238 μs, respectively. Longer fluorescence lifetime is good for energy storage.

In addition, the emission cross section can be estimated by the Fuchtbauer–Ladenburg formula[14]

$$\sigma_e(\lambda) = \frac{\lambda^4 \beta}{8\pi c n^2 \tau_r} \times \frac{\lambda I(\lambda)}{\int \lambda I(\lambda) \mathrm{d}\lambda}, \tag{2}$$

where λ is the wavelength, $I(\lambda)$ is the fluorescence intensity at wavelength λ, n is the refractive index of the Nd:LuAG ceramic, c is the speed of light in a vacuum, β is the branching ratio which is calculated based on Judd–Ofelt (J–O) theory, and τ_r is the radiative lifetime. The values of β and τ_r are shown in Table 1.

The emission cross section for the $^4F_{3/2} \rightarrow {}^4I_{11/2}$ transitions was calculated to be 9.77×10^{-20} cm^2 at 1066 nm. According to the formula $E_s = h\nu/\sigma$, where E_s is the saturation fluence, $h\nu$ is the photon energy, and σ is the emission cross section, we can get that E_s of the Nd:LuAG ceramic is 1.91 J/cm^2, which is much larger than that of Nd:YAG (0.67 J/cm^2). Large saturation fluence is also useful for energy storage. Therefore, Nd:LuAG ceramic is a good gain medium for high-energy lasers.

The size of Nd:LuAG ceramic used in our work is 3 mm × 3 mm × 8.5 mm with 1% doped. Both faces of the Nd:LuAG ceramic were anti reflect (AR)-coated at 808 and 1064 nm. As an illustration of the laser potential of Nd:LuAG ceramic, the CW and E-O Q-switch laser experiment were realized. The laser experiment was carried in a plane-parallel resonator shown in Fig. 3. In the CW mode, the E-O Q-switch (the polarizer, $\lambda/4$ waveplate and pockets cell) was taken away from the cavity. The length of the cavity is 50 mm. The mirror M1 is AR-coated at 808 nm and high-reflection-coated at 1064 nm. The mirror

Table 1. $^4F_{3/2}$ Level of Nd:LuAG

Transition from $^4F_{3/2}$	λ (nm)	β (%)	T_r (μs)
$^4I_{9/2}$	890	33.87	303
$^4I_{11/2}$	1066	53.72	
$^4I_{13/2}$	1339	11.85	
$^4I_{15/2}$	1880	0.56	

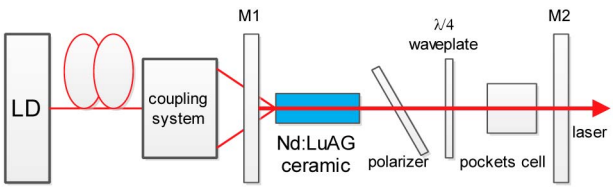

Fig. 3. Optical schematic of the laser system.

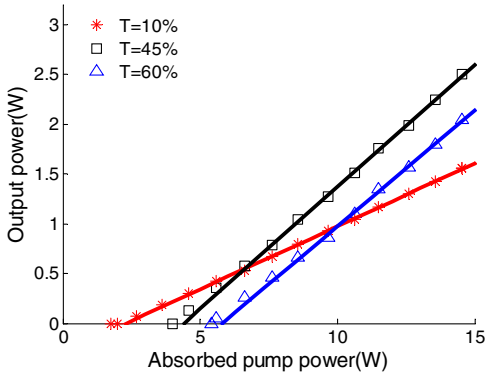

Fig. 4. Nd:LuAG ceramic CW laser output power versus absorbed pump power with different output transmissions.

M2 is selected to be output coupler with different transmission rates of 10%, 45%, and 60% at 1064 nm. Nd:LuAG ceramic output power versus the absorbed pump power and different transmission rates of the output couplers, as shown in Fig. 4. When the pump power was increased to 14.54 W, the maximum CW laser output of 2.5 W was obtained at the transmission rate of 45%, corresponding to optical conversion efficiency of 17.2% and slope efficiency of 24.3%.

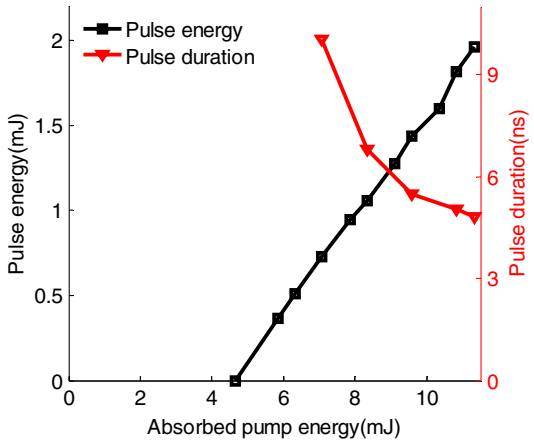

(a)

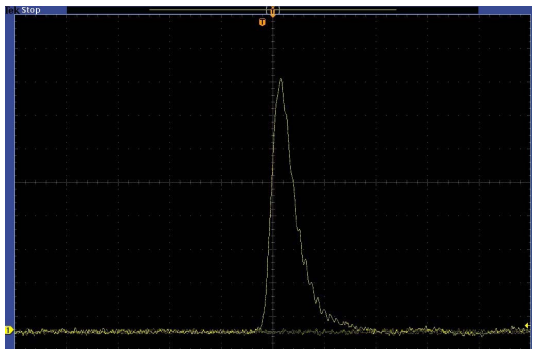

(b)

Fig. 5. (a) Pulse energy and pulse duration versus absorbed pump energy; (b) oscillogram of single pulse in Q-switching operation at maximum energy output.

We also got Q-switched laser output when the E-O Q-switch was inserted into the cavity. The cavity length is 175 mm with 60% transmission output coupler. The E-O Q-switched experimental setup is also illustrated as Fig. 3. Stable operation was achieved with the repetition rate of 1 Hz.

The output pulse energy and duration as a function of absorbed pump energy are shown in Fig. 5(a). A maximum output pulse energy of 1.96 mJ was achieved at the absorbed pump energy of 11.3 mJ, corresponding to an optical–optical conversion efficiency of 17.3% and a slope efficiency of 28.7%. The output pulse energy scaled linearly with the increase of pump energy. The oscillogram of pulse shape is shown in Fig. 5(b). We can see that the pulse duration is 4.8 ns.

In order to compare with the single-crystal rod laser, a 0.2%-doped Nd:LuAG crystal with dimensions 3 mm × 3 mm × 15 mm was placed in the cavity at the same pumping condition and experimental setup. The relation between single pulse energy and absorbed pump energy is shown in Fig. 6. When the absorbed pump energy is 8.08 mJ, the pulse energy of Nd:LuAG crystal is 2.05 mJ. Because of the scattering loss, the pulse energy of Nd:LuAG ceramic (1 mJ) is smaller than that of Nd:LuAG crystal. Although the laser efficiency of the Nd:LuAG ceramic laser is still less than that of the Nd:LuAG single-crystal laser, it shows the possibility of being used in high-energy laser in the near future. To

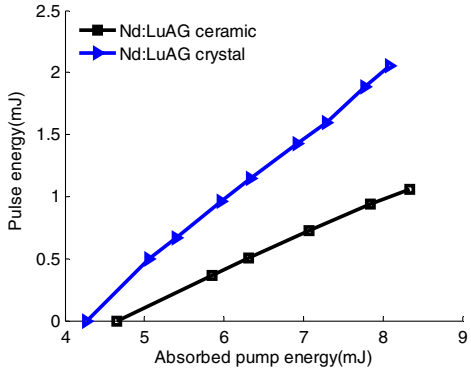

Fig. 6. Pulse energy versus absorbed pump energy.

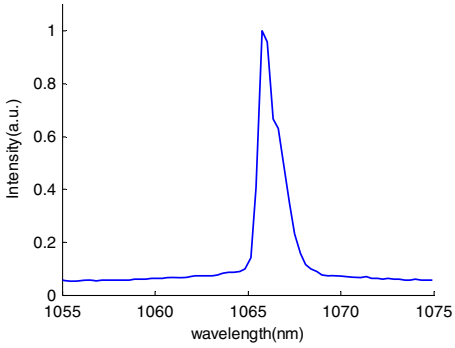

Fig. 7. Laser spectrum of Nd:LuAG ceramic.

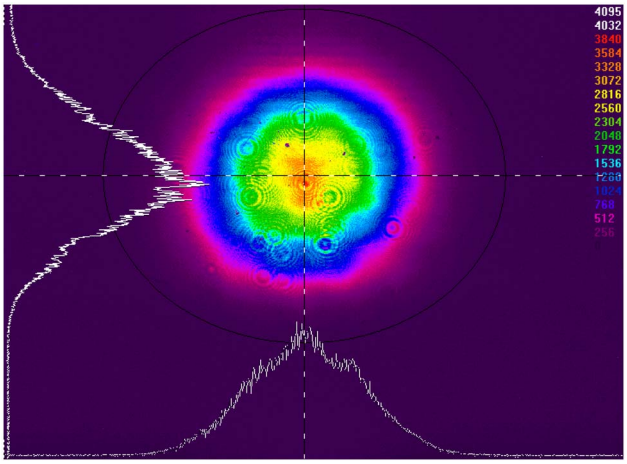

Fig. 8. Spatial distribution of the laser beam in near-field.

improve the optical quality of Nd:LuAG ceramic and try to get the same laser efficiency with single-crystal laser in high-energy field is our next step.

A spectrometer (Ocean Optics USB2000) is used to measure the output spectrum (Fig. 7). The central lasing wavelength is approximately 1066 nm, and the spectral width is 1.5 nm.

Figure 8 shows the near-field beam profile of the laser beam, which was measured at a pumped power of 0.5 W for Nd:LuAG ceramic. The laser was operated in long-pulse mode (10 Hz, 1000 μs). The spots and annuluses are caused by the dust on the CCD window glass surface. The intensity distribution of the beam profile possesses good symmetry.

In conclusion, the performance of CW and pulse operation of Nd:LuAG ceramic laser is experimentally studied. We believe that Nd:LuAG ceramics as a new generation of laser materials will become a very good alternative to widely used Nd:YAG single crystals for Q-switch lasers. Nd:LuAG ceramics is also a potential gain material which can be applied to IFE.

We thank Peixiong Zhang for providing the Nd:LuAG crystal for us.

†These authors contributed equally to this work and share first authorship.

References

1. E. Auffray, D. Abler, S. Brunner, B. Frisch, A. Knapitsch, P. Lecoq, G. Mavromanolakis, O. Poppe, and A. Petrosyan, in *Nuclear Science Symposium Conference Record (NSS/MIC)* (IEEE, 2009), pp. 2245.
2. D. C. Brown, C. D. McMillen, C. Moore, J. W. Kolis, and V. Envid, J. Lumin. **148**, 26 (2014).
3. X. Xu, X. Wang, J. Meng, Y. Cheng, D. Li, S. Cheng, F. Wu, Z. Zhao, and J. Xu, Laser Phys. Lett. **6**, 678 (2009).
4. J. Di, X. Xu, W. Tan, J. Zhang, D. Tang, D. Li, D. Zhou, F. Wu, and J. Xu, Laser Phys. Lett. **10**, 095801 (2013).
5. X. Xu, J. Di, W. Tan, J. Zhang, D. Tang, D. Li, D. Zhou, and J. Xu, Laser Phys. Lett. **9**, 406 (2012).
6. J. Zhao, S. Zhao, K. Yang, L. Zheng, and J. Xu, Laser Phys. Lett. **10**, 055806 (2013).
7. A. Ikesue, I. Furusato, and K. Kamata, J. Am. Ceram. Soc. **78**, 225 (1995).
8. J. Chen, J. Li, J. Xu, W. Liu, Y. Bo, X. Feng, Y Xu, D. Jiang, Z. Chen, Y. Pan, Y. Guo, B. Yan, C. Guo, L. Yuan, H. Yuan, Y. Lin, Y. Xiao, Q. Peng, W. Lei, D. Cui, and Z. Xu, Opt. Laser Technol. **63**, 50 (2014).
9. J. Kawanaka, N. Miyanaga, T. Kawashima, K. Tsubakimoto, Y. Fujimoto, H. Kubomura, S. Matsuoka, T. Ikegawa, Y. Suzuki, N. Tsuchiya, T. Jitsuno, H. Furukawa, T. Kanabe, H. Fujita, K. Yoshida, H. Nakano, J. Nishimae, M. Nakatsuka, K. Ueda, and K. Tomabechi, J. Phys. **112**, 032058 (2008).
10. H. Yang, J. Meng, X. Ma, and W. Chen, Chin. Opt. Lett. **12**, 121406 (2014).
11. S. Li, X. Ma, H. Li, F. Li, X. Zhu, and W. Chen, Chin. Opt. Lett. **11**, 071402 (2013).
12. C. Zhou, Y. Liu, R. Zhou, S. Du, X. Hou, and W. Chen, Chin. Opt. Lett. **11**, 081403 (2013).
13. Y. Zhang, M. Cai, B. Jiang, J. Fan, C. Zhou, X. Mao, and L. Zhang, Opt. Mater. Express **4**, 2182 (2014).
14. B. F. Aull and H. Jenssen, IEEE J. Quantum Electron. **18**, 925 (1982).